

Short Communication

## Oriented texture of Y-doped $\text{La}_{10}\text{Si}_6\text{O}_{27}$ Ceramic prepared by rapid solidification method

Dechuan Li<sup>1\*</sup>, Mingyu Li<sup>2</sup>, Yongxing Zhang<sup>1</sup>, Guangping Zhu<sup>1</sup>, Xude Wang<sup>1</sup>

<sup>1</sup> School of Physics & Electronic Information, Huaibei Normal University, Huaibei, 235000, China

<sup>2</sup> Department of mathematics and physics, Zhengzhou Institute of Aeronautical Industry Management, Zhengzhou, 450046, China

\*E-mail: [dchli@qq.com](mailto:dchli@qq.com)

Received: 30 July 2016 / Accepted: 21 September 2016 / Published: 10 November 2016

Oriented texture  $\text{La}_{9.33}\text{Y}_{0.67}\text{Si}_6\text{O}_{27}$  ceramic was successfully synthesized by laser rapid solidification method. The  $\text{La}_{9.33}\text{Y}_{0.67}\text{Si}_6\text{O}_{27}$  crystal was formed only after Yttrium was added into the  $\text{La}_{10}\text{Si}_6\text{O}_{27}$  ceramic under the sintering of  $\text{CO}_2$  continuous wave laser. As for pure  $\text{La}_{10}\text{Si}_6\text{O}_{27}$ , the oriented texture ceramic could not be sinterable directly. Even the  $\text{La}_{10}\text{Si}_6\text{O}_{27}$  preparing by high temperature solid state reaction begins to decompose under laser sintering. The result shows that the suitable sintering laser power of texture  $\text{La}_{9.33}\text{Y}_{0.67}\text{Si}_6\text{O}_{27}$  ceramic is 400W. Thermal expansion coefficient of  $\text{La}_{9.33}\text{Y}_{0.67}\text{Si}_6\text{O}_{27}$  is  $7.71 \times 10^{-6} \text{ K}^{-1}$ ,  $7.76 \times 10^{-6} \text{ K}^{-1}$  and  $7.83 \times 10^{-6} \text{ K}^{-1}$  at 600°C, 650°C and 700°C, respectively. The cell with textured  $\text{La}_{9.33}\text{Y}_{0.67}\text{Si}_6\text{O}_2$  shows a better output power density than that of  $\text{La}_{10}\text{Si}_6\text{O}_{27}$ . The data suggest that the texture and lower thermal expansion  $\text{La}_{9.33}\text{Y}_{0.67}\text{Si}_6\text{O}_{27}$  ceramic could be prepared by Yttrium substitution using laser sintering for the high oxide ion conduction.

**Keywords:** Ceramic; Texture; Laser sintering; Lanthanum silicate; Thermal expansion coefficient

### 1. INTRODUCTION

Apatite is a kind of material that has oxide ionic conductivity for the electrolyte of solid oxide fuel cells. Among the lanthanum silicate-based apatite,  $\text{La}_{10}\text{Si}_6\text{O}_{27}$  has the high conductivity than yttria doped zirconia in the intermediate temperature operating condition. Moreover, the oxygen ion transference number is relatively high over a wide range of oxygen partial pressure for fuel cells [1-3]. The high ionic conduction is attributed to the oxide ions located at the 2a site of the channel, which is the key mechanism of oxide ionic conduction for the anisotropy ceramic [4]. Few grain boundary of ceramic is helpful to decrease the resistance of oxygen ionic conduction. Therefore, pure phase and oriented growth ceramics are two essential factors to improve the oxide ionic conductivity. In fact, the

high temperature is needed for the preparation of  $\text{La}_{10}\text{Si}_6\text{O}_{27}$ . According to the previous report by Nakayama et al. [5],  $\text{La}_{10}\text{Si}_6\text{O}_{27}$  was synthesized by solid reaction method sintered at 1700-1800°C. Using a suitable thermal pretreatment, the sintering temperature could be reduced to 1600°C [6]. Even taking the water-based gel-casting technique, the synthesis temperature of  $\text{La}_{10}\text{Si}_6\text{O}_{27}$  could be descended to 1550°C [7]. Additionally, the secondary phase is generated frequently in the synthesized process. The formation of the second phase is unfavorable because the ceramic might be destroyed by the reaction between the compound and  $\text{H}_2\text{O}$  or  $\text{CO}_2$ . Besides, the impurity phase could greatly retard the oxygen ion conduction [8-10]. Itagkai et al reported that the minor phase of  $\text{La}_2\text{SiO}_5$  could be reduced by Li-doping in lanthanide silicate, which is existed at the grain boundaries [11]. On the other hand, the preparation of oriented growth ceramic with few grain boundary is an efficient method to improve the oxygen ion transportation. Tao et al indicated that the grain boundary resistance is dominant in the impedance spectrum for conductivity [12]. Nakayama et al investigated the oxygen ionic conductivity of  $\text{Nd}_{9.33}(\text{SiO}_4)\text{O}_2$  single crystal, and founded that the conductivity value parallel to c-axis is higher about ten times than the value perpendicular to c-axis in an anisotropy crystal [13]. Oriented ceramic has more advantage than isotropic ceramic in ionic conduction. Therefore, it is more significant to find a better synthesis method for obtaining pure and oriental grown lanthanum silicate ceramic.

In current work, we prepared the oriented texture  $\text{La}_{9.33}\text{Y}_{0.67}\text{Si}_6\text{O}_{27}$  ceramic by laser rapid solidification method. This texture ceramic has larger grain. Few grain boundaries of this texture ceramic have the great advantage in conducting oxygen ion. On the other hand, La and Y could take the site in each other crystal lattice in Lanthanum silicate. Y doped  $\text{La}_{10}\text{Si}_6\text{O}_{27}$  could not introduce the second phase at the grain boundary to increase the grain boundary resistance. Hence, we evaluate the synthesis, character and thermal expansion of pure oriented  $\text{La}_{9.33}\text{Y}_{0.67}\text{Si}_6\text{O}_{27}$  ceramics by laser rapid solidification method.

## 2. EXPERIMENT

The  $\text{La}_{9.33}\text{Y}_{0.67}\text{Si}_6\text{O}_{27}$  and  $\text{La}_{10}\text{Si}_6\text{O}_{27}$  were synthesized by rapid solidification method in 2 min. High purity  $\text{La}_2\text{O}_3$ ,  $\text{Y}_2\text{O}_3$ ,  $\text{SiO}_2$  were used as reagents. Steel was used for the support of ceramic during the laser sintering, which is a critical factor for its high thermal conductivity in the process of ceramic oriented crystallization. Laser sintering was carried out by a 5 kW continuous wave  $\text{CO}_2$  laser. The pellet was exposed to the laser beam of 5mm in diameter. Before weighing,  $\text{La}_2\text{O}_3$  and  $\text{Y}_2\text{O}_3$  were calcined at 1000°C for 6h, then ground with  $\text{SiO}_2$  for 4h in agate mortar. The mixtures were uniaxially pressed into a circular mold ( $\varnothing=14\text{mm}$ ) under a pressure of 400Mpa for 2 min. The green pellets were put on the steel plate, and then the laser beam was moved on the age of the pellet. The whole pellet would melt completely, and then holds the beam on it for 2min with the power between 400W and 1000W in the interval of 200W. Finally, turn down the laser power slowly.  $\text{La}_{10}\text{Si}_6\text{O}_{27}$  has also been prepared by solid reaction method at 1600°C (6h) for comparison. We also took the sintered  $\text{La}_{10}\text{Si}_6\text{O}_{27}$  prepared by solid reaction method under laser sintering.

The crystal structures of powders were characterized by X-ray diffraction (PANalytical B.V.) using an X'pert PRO diffractometer and Cu K $\alpha$  radiation in the  $2\Theta$  range of 10-80°. Scanning electron microscopy (SEM) (JSM-6700F) was employed to examine the morphology of the fracture of the sample. The linear thermal expansion coefficient (TEC) was measured on the thermal expansion apparatus (LINSEIS DIL L76) using quartz as the reference material with a heating rate of 5°C per min from room temperature to 800°C. The electrochemical performances were tested by a PARSTAT 2273 (Princeton, USA) at 600°C.

### 3. RESULTS AND DISCUSSION

#### 3.1 The influence of Y doping on the stability of $\text{La}_{9.33}\text{Y}_{0.67}\text{Si}_6\text{O}_{27}$

In this experiment, we investigated whether the pure  $\text{La}_{10}\text{Si}_6\text{O}_{27}$  was prepared by rapid solidification method. Figure 1(a) shows the X-ray powder diffraction patterns of  $\text{La}_{10}\text{Si}_6\text{O}_{27}$  powders by CO<sub>2</sub> laser sintering between 400W and 1000W. According to the major phase, all five samples exhibit an apatite structure (JCPDS: 00-053-0291). The secondary phases  $\text{La}(\text{OH})_3$  and  $\text{SiO}_2$  were also detected. The existence of  $\text{La}(\text{OH})_3$  was the result of reaction between  $\text{La}_2\text{O}_3$  and  $\text{H}_2\text{O}$  in atmosphere. The interesting thing is that the impure  $\text{La}_{10}\text{Si}_6\text{O}_{27}$  bulk would decompose into pieces especially in wet atmosphere after 12h, which is different from ceramic prepared by solid reaction. The laser power densities corresponding with laser power were listed in Table 1. Even when the pure  $\text{La}_{10}\text{Si}_6\text{O}_{27}$  prepared by solid reaction method at 1600°C (6h) was sintered again by laser, the sintered ceramic was also cracked as before.

Figure 1(b) shows XRD patterns of  $\text{La}_{9.33}\text{Y}_{0.67}\text{Si}_6\text{O}_{27}$  sintering by CO<sub>2</sub> laser between 400W and 1300W and diffraction data of the apatite  $\text{La}_{10}\text{Si}_6\text{O}_{27}$  (JCPDS: 53-291). It can be seen that apatite phases have been formed under the power of 1000W. When the laser power was high than 1300W, the peak of  $\text{La}(\text{OH})_3$  was observed obviously in the XRD pattern. The minor phase would make the bulk ceramic decompose into pieces because the water was absorbed by  $\text{La}_2\text{O}_3$ . It might be related to the vapor of  $\text{SiO}_2$  under high power density.

As is shown in Figure 2(a), the bulk  $\text{La}_{10}\text{Si}_6\text{O}_{27}$  ceramic was decomposed into the mass of strip grains. However, in Figure 2(b), the crystal growth was highly oriented along the laser incident direction from the bottom to surface for  $\text{La}_{9.33}\text{Y}_{0.67}\text{Si}_6\text{O}_{27}$ . The distinctive crystal solidified process is a great temperature gradient of material with fast cooling rate from liquid to solid [14, 15]. The grains are over 50  $\mu\text{m}$  in diameter and much greater than other prepared method, such as sol-gel process [16, 17]. The bigger grain of laser rapid solidification ceramic will be more benefit to improve the oxygen ion conductivity with few grain boundaries.

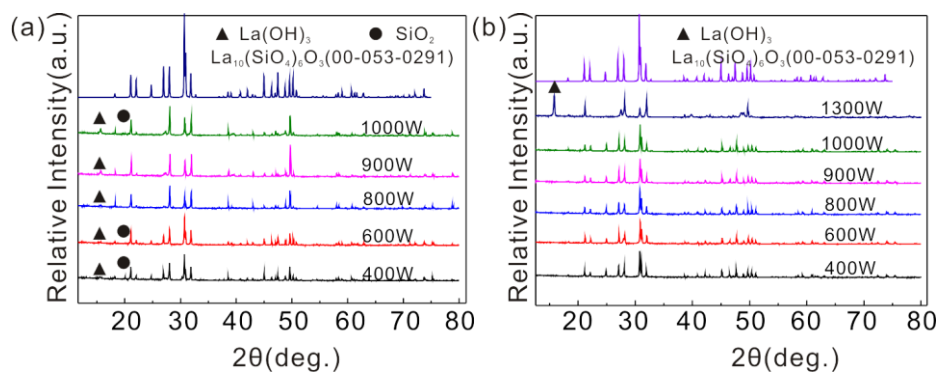


**Figure 1.** XRD patterns of (a)  $\text{La}_{10}\text{Si}_6\text{O}_{27}$ ; (b)  $\text{La}_{9.33}\text{Y}_{0.67}\text{Si}_6\text{O}_{27}$  ceramic sintered by  $\text{CO}_2$  laser with different irradiation of laser power.

**Table 1.** Laser power and corresponding laser power density irradiate on samples

Power (W)	400	600	800	900	1000	1300
Power density ( $\text{W cm}^{-2}$ )	509	764	1019	1146	1273	1656

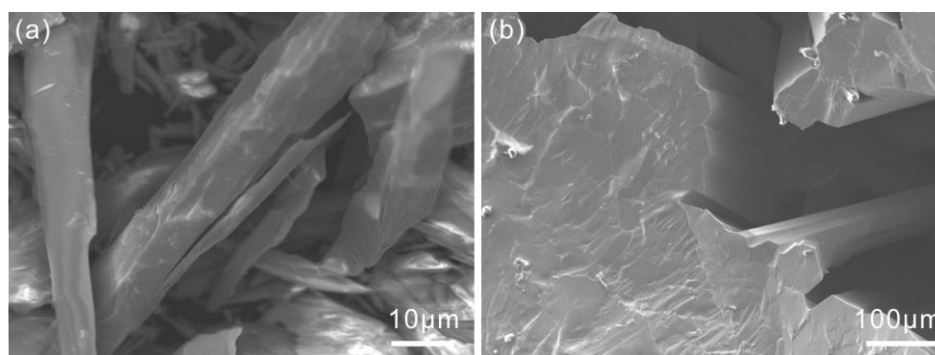


**Figure 2.** SEM images of ceramic sintered by  $\text{CO}_2$  laser: (a)  $\text{La}_{10}\text{Si}_6\text{O}_{27}$  sintered at 1000W; (b)  $\text{La}_{9.33}\text{Y}_{0.67}\text{Si}_6\text{O}_{27}$  sintered at 400W.

3.2 Thermal expansion analysis of  $\text{La}_{9.33}\text{Y}_{0.67}\text{Si}_6\text{O}_{27}$

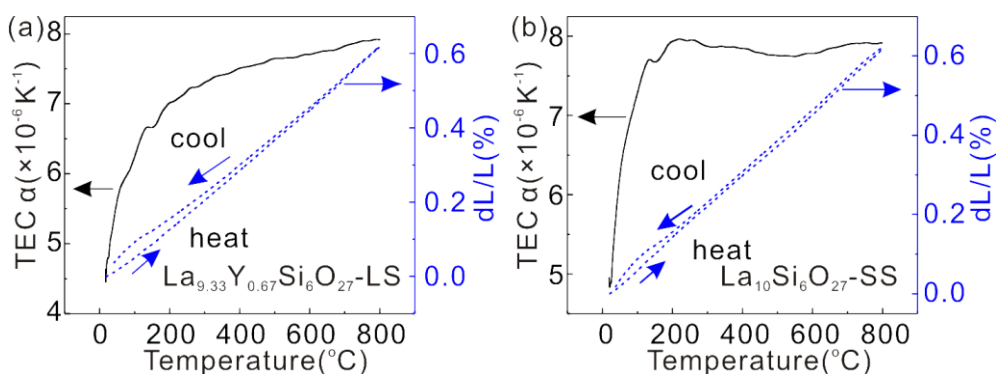


**Figure 3.** Thermal expansion curve (solid line) and relative length variation (dash line) of ceramic: (a)  $\text{La}_{9.33}\text{Y}_{0.67}\text{Si}_6\text{O}_{27}$  by laser sintering at 400W; (b)  $\text{La}_{10}\text{Si}_6\text{O}_{27}$  by solid reaction method at  $1600^\circ\text{C}$  (6h)

Figure 3 shows the thermal expansion curves of  $\text{La}_{9.33}\text{Y}_{0.67}\text{Si}_6\text{O}_{27}$  and  $\text{La}_{10}\text{Si}_6\text{O}_{27}$  with the heat data. The  $\text{La}_{9.33}\text{Y}_{0.67}\text{Si}_6\text{O}_{27}$  exhibited high orientation and similar thermal expansion with the  $\text{La}_{10}\text{Si}_6\text{O}_{27}$ . The maximum TEC value is  $7.91 \times 10^{-6} \text{K}^{-1}$  at  $800^\circ\text{C}$  for  $\text{La}_{9.33}\text{Y}_{0.67}\text{Si}_6\text{O}_{27}$ , which is approximate to the report [18]. The TEC value of this texture  $\text{La}_{9.33}\text{Y}_{0.67}\text{Si}_6\text{O}_{27}$  ceramic is smaller than  $9.7 \times 10^{-6} \text{K}^{-1}$  for  $\text{La}_{10}\text{Si}_6\text{O}_{27}$ ,  $10.0 \times 10^{-6} \text{K}^{-1}$  for YSZ and  $11.8 \times 10^{-6} \text{K}^{-1}$  for GDC [7]. Ou et al also report that Cu-doped  $\text{La}_{10}\text{Si}_{6-x}\text{Cu}_x\text{O}_{27-\delta}$  shows approximately TEC values of  $8.8\text{--}9.1 \times 10^{-6} \text{K}^{-1}$  at  $25\text{--}800^\circ\text{C}$  [19]. The TEC value of the texture ceramic increased gently with the temperature elevated, which might be more suitable for the electrolyte to match cathode and anode components of solid state fuel cells.

### 3.3 Cell performance

A single fuel cell of cathode| $\text{La}_{9.33}\text{Y}_{0.67}\text{Si}_6\text{O}_{27}$ |anode was fabricated to evaluate the electrochemical performance. The thickness of the electrolyte was set to 1.5mm. The composite cathode was prepared by BSBCF and  $\text{La}_{9.33}\text{Y}_{0.67}\text{Si}_6\text{O}_{27}$  with the mixed weight ratio of 60:40. The NiO-Sm doped  $\text{CeO}_2$  (70:30 wt%) was used for fuel cell anode. The calcined temperature of cathode and anode painted materials was  $1100^\circ\text{C}$  for 4h and  $1400^\circ\text{C}$  for 4h, respectively. For a single fuel cell, the fuel was  $\text{H}_2$  and the cathode was exposed to the air. Figure 4 shows the electrochemical performance of a single cell at  $600^\circ\text{C}$ . For comparison, the cell of cathode| $\text{La}_{10}\text{Si}_6\text{O}_{27}$ |anode was also fabricated. From the image, the open circuit voltage is approximately 1V for both texture  $\text{La}_{9.33}\text{Y}_{0.67}\text{Si}_6\text{O}_{27}$  ceramic and  $\text{La}_{10}\text{Si}_6\text{O}_{27}$  (solid reaction method at  $1600^\circ\text{C}$ , 6h) corresponding to the high oxide ion conductivity of lanthanum silicate [17, 18, 20].

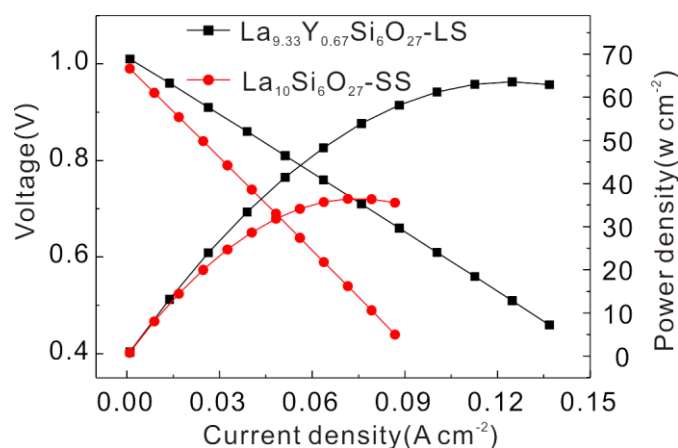


**Figure 4.** Cell voltage and power density of an electrolyte:  $\text{La}_{9.33}\text{Y}_{0.67}\text{Si}_6\text{O}_{27}$  (laser sintering, LS) and  $\text{La}_{10}\text{Si}_6\text{O}_{27}$  (solid state reaction, SS)

From the I-P curve of the single cell, peak power densities were  $36.5 \text{ mW cm}^{-2}$  for the cell with  $\text{La}_{10}\text{Si}_6\text{O}_{27}$  electrolyte and  $63.6 \text{ mW cm}^{-2}$  for the cell with texture  $\text{La}_{9.33}\text{Y}_{0.67}\text{Si}_6\text{O}_{27}$  ceramic at  $600^\circ\text{C}$ . However, the electrolyte is relatively thick which prevents the increasing output of power density. But we still could deduce that the cell with textured  $\text{La}_{9.33}\text{Y}_{0.67}\text{Si}_6\text{O}_{27}$  shows a better output power density than that of  $\text{La}_{10}\text{Si}_6\text{O}_{27}$ . This textured structure provides a channel for the migration of oxide ions in

the oxide ion conductor [21]. It is important to improve the oxide ion conductivity by reducing the resistance of the grain boundary than polycrystalline ceramic [7, 10]. The electrochemical performance of textured ceramic sintered by laser is excellent. The character of oxygen ion conduction is approximately for the sample prepared by floating zone method [13, 21]. The cell performance suggests that the textured  $\text{La}_{9.33}\text{Y}_{0.67}\text{Si}_6\text{O}_{27}$  is a better electrolyte material for solid oxide fuel cells.

#### 4. CONCLUSION

Y doped  $\text{La}_{9.33}\text{Y}_{0.67}\text{Si}_6\text{O}_{27}$  oriented ceramic was successfully prepared by laser rapid solidification in two minutes with a  $\text{CO}_2$  laser. However, when the laser was applied into the  $\text{La}_{10}\text{Si}_6\text{O}_{27}$ , the pure  $\text{La}_{10}\text{Si}_6\text{O}_{27}$  could not be gained even at higher laser power density of  $1656 \text{ W cm}^{-2}$ , which is mixed with the  $\text{La}_2\text{O}_3$  impurity. Texture  $\text{La}_{10}\text{Si}_6\text{O}_{27}$  ceramic could not be prepared directly by laser rapid solidification method. The TEC of  $\text{La}_{9.33}\text{Y}_{0.67}\text{Si}_6\text{O}_{27}$  (laser rapid solidification) is similar to that of  $\text{La}_{10}\text{Si}_6\text{O}_{27}$  (solid reaction method). TEC values are  $7.71$ ,  $7.83$  and  $7.91 \times 10^{-6} \text{ K}^{-1}$  at  $600$ ,  $700$  and  $800^\circ\text{C}$ , respectively. The fuel cell with texture  $\text{La}_{9.33}\text{Y}_{0.67}\text{Si}_6\text{O}_{27}$  shows better electrochemical performance than that of  $\text{La}_{10}\text{Si}_6\text{O}_{27}$ . The improvement oxide ion conductivity may be ascribed to the decrease of grain boundary resistance and advantaged texture structure in the process of oxygen ion conduction.

#### ACKNOWLEDGEMENTS

This work was financially supported by the National Natural Science Foundation of China (51302102, 11504121), Natural Science Research Project for Colleges and Universities of Anhui Province (KJ2014B02, KJ2016A638), and the Huaibei Scientific Talent Development Scheme (20140305).

#### References

1. H. Arikawa, H. Nishiguchi, T. Ishihara, Y. Takita, *Solid State Ionics*, 136 (2000) 31.
2. H. Yoshioka, S. Tanase, *Solid State Ionics*, 176 (2005) 2395.
3. M.Y. Gorshkov, A.D. Neumin, N.M. Bogdanovich, Y.V. Danilov, L.A. Dunyushkina, *Russ. J. Electrochem.*, 43 (2007) 721.
4. S. Nakayama, M. Sakamoto, M. Highchi, K. Kodaira, *J Mater Sci Lett*, 19 (2000)91.
5. S. Nakayama, M. Sakamoto, *J. Eur. Ceram. Soc.*, 18 (1998) 1413.
6. Y.L. Kuo, Y.Y. Liang, *Ceram. Int.*, 38 (2012) 3955.
7. S.P. Jiang, L. Zhang, H.Q. He, K.Y. Rong, Y. Xiang, *J. Power Sources*, 189 (2009) 972.
8. S. Hwan Jo, P. Muralidharan, D.K. Kim, *J. Mater. Res.*, 24 (2009) 237.
9. A.L. Shaula, V.V. Kharton, F.M.B. Marques, *Solid State Ionics*, 177 (2006) 1725.
10. J. Xiang, Z.G. Liu, J.H. Ouyang, F.Y. Yan, *Ceram. Int.*, 40 (2014) 2401.
11. Y. Itagaki, N. Takeda, Y. Sadaoka, *Ecs Transactions*, 16 (2008) 539.
12. S. Tao, J.T.S. Irvine, *Mater. Res. Bull.*, 36 (2001) 1245.
13. S. Nakayama, M. Sakamoto, M. Higuchi, K. Kodaira, M. Sato, S. Kakita, T. Suzuki, K. Itoh, *J. Eur. Ceram. Soc.*, 19 (1999) 507.
14. J.M. Yu, M.J. Chao, D.C. Li, M.Y. Li, *J. Power Sources*, 226 (2013) 334.
15. J.J. Zhang, J.M. Yu, M.J. Chao, E.J. Liang, M.Y. Li, D.C. Li, *J. Mater. Sci.*, 47 (2012) 1554.
16. X.G. Cao, S.P. Jiang, Y.Y. Li, *J. Power Sources*, 293 (2015) 806.

17. D.D.Y. Setsoafia, P. Hing, S.C. Jung, A.K. Azad, C.M. Lim, *Solid State Sci.*, 48 (2015) 163.
18. J. Xiang, Z.G. Liu, J.H. Ouyang, F.Y. Yan, *J. Power Sources*, 251 (2014) 305.
19. X.F. Ding, G.X. Hua, D. Ding, W.L. Zhu, H.J. Wang, *J. Power Sources*, 306 (2016) 630.
20. G. Ou, X.R. Ren, L. Yao, H. Nishijima, W. Pan, *J. Mater. Chem. A*, 2 (2014) 13817.
21. M. Higuchi, Y. Masubuchi, S. Nakayama, S. Kikkawa, K. Kodaira, *Solid State Ionics*, 174 (2004) 73.

© 2016 The Authors. Published by ESG ([www.electrochemsci.org](http://www.electrochemsci.org)). This article is an open access article distributed under the terms and conditions of the Creative Commons Attribution license (<http://creativecommons.org/licenses/by/4.0/>).